RESOLUTION IN ELECTRON MICROSCOPE RADIOAUTOGRAPHY

M. M. SALPETER, L. BACHMANN, and E. E. SALPETER

From the Department of Applied Physics and the Section of Neurobiology and Behavior, and the Laboratory of Nuclear Studies, Cornell University, Ithaca, New York 14850, and the Institute for Physical Chemistry, University of Innsbruck, Austria. Dr. Bachmann's present address is the Institut für Technische Chemie, Technische Hochschule, Munich, Germany

ABSTRACT

An analysis of grain distributions around a radioactive line source (consisting of polystyrene-^{3}H) showed that the shape of the distribution was independent of the factors that influence resolution, i.e. section and emulsion thickness, silver halide crystal, and developed grain size. These factors did effect the spread of the distribution, however, and thus the distance from the line source within which 50% of the total developed grains fell. We called this distance "half distance" (HD) and determined it for a variety of specimens. When grain distributions were normalized in units of HD, one could plot universal grain distributions for specimens with radioactive sources of various shapes. The use of HD and the universal curves in interpreting radioautograms is discussed.

I. INTRODUCTION

Electron microscope (EM) radiaoutography introduced by Liquier-Milward (1956) is now used routinely in many laboratories. Most of the technical difficulties in specimen preparation have been overcome (see Caro and Van Tubergen, 1962; Salpeter and Bachmann, 1964, 1965; Salpeter, 1966; Stevens, 1966). The shortcomings now lie mainly in the analytical end of the procedure. A full interpretation of radioautograms depends on a knowledge of the expected grain distribution around radioactive sources. Several discussions (Caro, 1962; Pelc, 1963; Granboulan, 1963; Bachmann and Salpeter, 1965) have emphasized that this distribution depends both on geometric factors (i.e. section and emulsion thickness, electron scattering) and on photographic ones (i.e. diameter of both the silver halide crystals of the emulsion and the developed grain). For relevant studies on resolution in light microscope radioautography, see Doniach and Pelc (1950), Stevens (1950), and Lamerton and Harris (1954). However, one still needs systematic experimental investigations of the degree to which variations in these parameters effect the grain distribution, and thus the resolution, in EM radioautography. An important beginning was made by Caro, who obtained experimentally the grain distribution for one set of conditions of geometry and photography (Caro, 1962; Caro and Schnos, 1965).

The present paper has a threefold aim: (*a*) to describe a simple calibration specimen for testing resolution in electron microscope radioautography (Section II *a*), (*b*) to present experimental results giving the resolution of radioautographic preparations differing in geometric and photographic parameters (Section III), and (*c*) to provide information regarding expected grain distributions around radioactive sources of different shapes and sizes, which could be used by the reader in interpreting his own radioautograms (Section IV *b*).

By using radioactive line sources (Section II), we found that all the grain distributions for dif-

ferent radioautographic preparations could be characterized by a common "universal curve," although each had a different value for a length related to resolution, which we call the "half distance," HD (Section III). This universality enables us to infer mathematically the grain distribution around sources other than lines (Section IV *a*) and leads to the suggested applications in Section IV *b*.

II. MATERIALS AND METHODS

a. Specimen

A specimen which provided a radioactive line source was used. It consisted of a thin film of styrene-^{3}H approximately 500 A thick, which was sandwiched between Epon 812 and methacrylate and then sectioned at right angles. The styrene-^{3}H dissolved in benzene was obtained from New England Nuclear Corp. (Boston, Mass.) at initial specific activity of 5 c/mg. It was then mixed with nonradioactive styrene to final specific activities of 1 or 0.1 mc/mg. The benzene was evaporated, and the polymer was redissolved in amyl acetate. Thin uniform films of styrene were then formed on glass slides (as can be done with collodion). Each styrene film was measured interferometrically to determine its thickness and then was stripped onto a water surface. For support, the radioactive films were picked up on Epon "half blocks" (see Fig. 1), air dried, and covered by a layer of methacrylate. (Polymerized methacrylate, dissolved in chloroform and amyl acetate, also forms uniform films on glass slides.) The radioactive styrene film is thus sandwiched between Epon and methacrylate without ever coming in contact with the solvent systems usually employed in the procedure of embedding in plastic (see Fig. 1). When sectioned at right angles, the radioactive film appears as a line source approximately 500 A wide. The styrene line can clearly be seen in the electron microscope without additional staining (Fig. 2). We chose an artificial specimen rather than a biological one because the uniformity and specific activity of radioactivity can be better controlled. We chose a line source rather than a point source for greater ease in data collecting. One can calculate back theoretically from the distribution of developed grains around a line source to that around other sources, as shown in Section IV.

b. Experiment

Sections, both with grey and with medium gold interference colors, were cut at right angles through the hot film. The sections were mounted on collodion-coated slides for electron microscope radioautography, and their thickness was measured interferometrically with a Nomarski incident light interferometer. The "grey" sections ranged from 450 to 550 A with a mean at 500 A. The "medium gold" sections ranged from 1100 to 1250 A with a mean at 1200 A. These values were in agreement with the values published by Peachey (1958) and Bachmann and Sitte (1958). No staining was used. The sections were vacuum-coated with approximately 50 A of carbon and coated with a monolayer of Ilford L4, purple interference color (~1400 A), or with centrifuged Kodak NTE either as a monolayer, pale gold interference color (~700 A), or as a double layer, purple interference color (~1400 A). The standardization of this procedure has been described before (Salpeter and Bachmann, 1964, 1965; Bachmann and Salpeter, 1965, 1967). After about 1–2 wk of exposure, the slides were developed, the Ilford L4 with either Microdol X (Eastman Kodak Co., Rochester, N.Y.) or paraphenylenediamine, and Kodak NTE with either Dektol or gold latensification-Elon ascorbic acid (Salpeter and Bachmann, 1964). The developed radioautograms were photo-

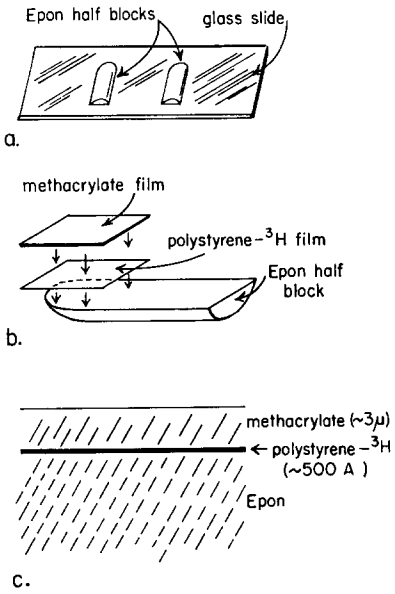

FIGURE 1 Specimen for obtaining radioactive hot line. *a*, Epon blocks, cut longitudinally, are placed, cut surface down, onto a drop of Epon 812 monomer on a glass slide. When the monomer is polymerized, a smooth surface is obtained on the half block. *b*, Thin film of polystyrene-^{3}H (~500 A) is formed on glass slide, floated on water, and picked up onto half block; a thicker layer of nonradioactive methacrylate (~3 μ) is similarly prepared and picked up over the polystyrene. *c*, Final specimen sandwich-sectioned at right angles to hot layer.

graphed along the full length of the hot line to avoid biasing the sampling. For each specimen enough line was photographed to yield over 1000 developed grains. The distance from the midpoint of every developed grain was measured to the middle of the hot line. (To determine a grain midpoint, a small plastic mask which had a series of concentric circles marked around a common perforated center was laid

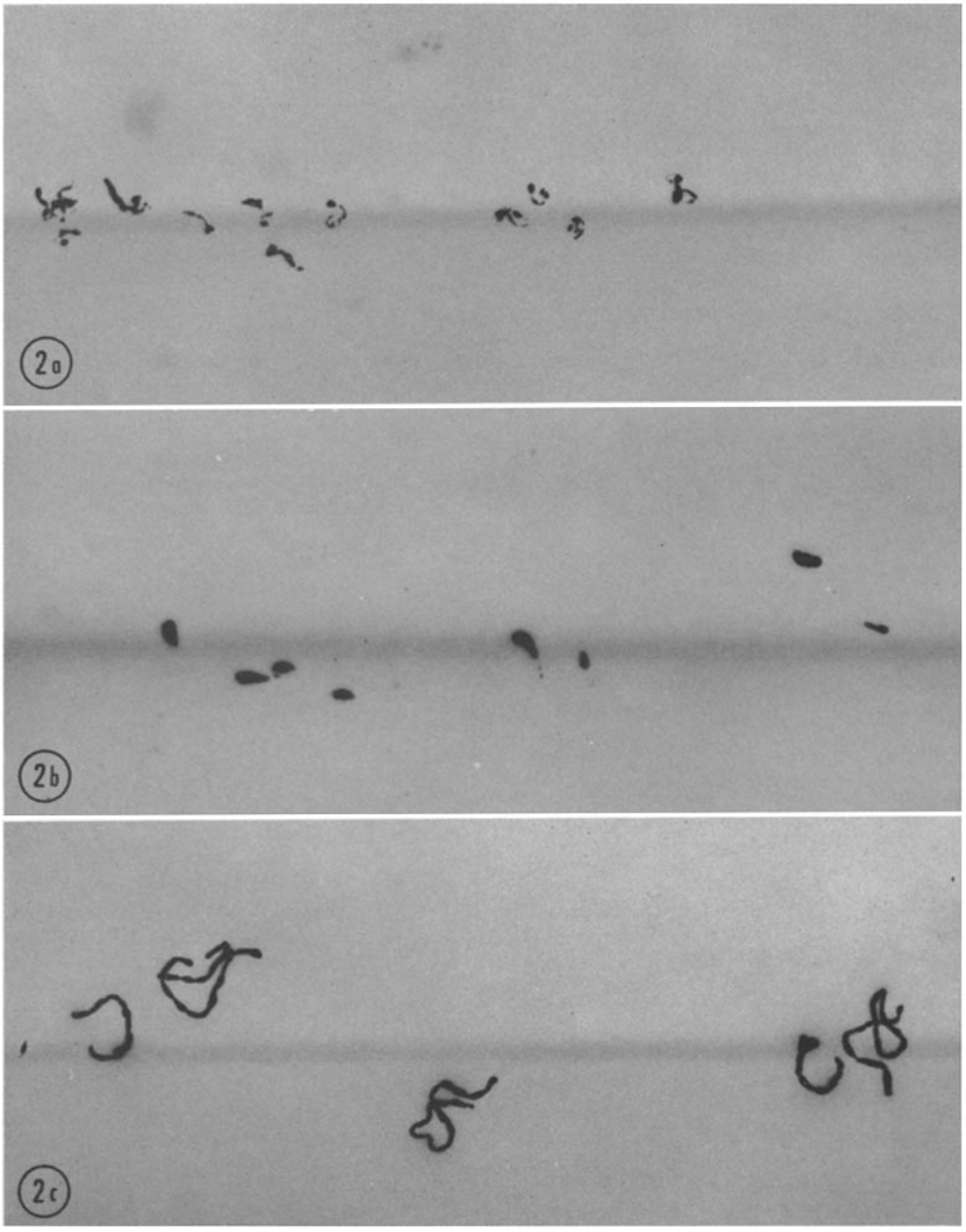

FIGURE 2 Radioactive "hot line," 500 A section (grey interference color). Emulsion somewhat oversaturated for better illustration. *a*, Coated with a monolayer of Kodak NTE and developed with Dektol (2 min). *b*, Coated with a monoalyer of Ilford L4 and developed with paraphenylenediamine (1 min). *c*, Coated with a monolayer of Ilford L4 and developed with Microdol X (3 min). × 45,000.

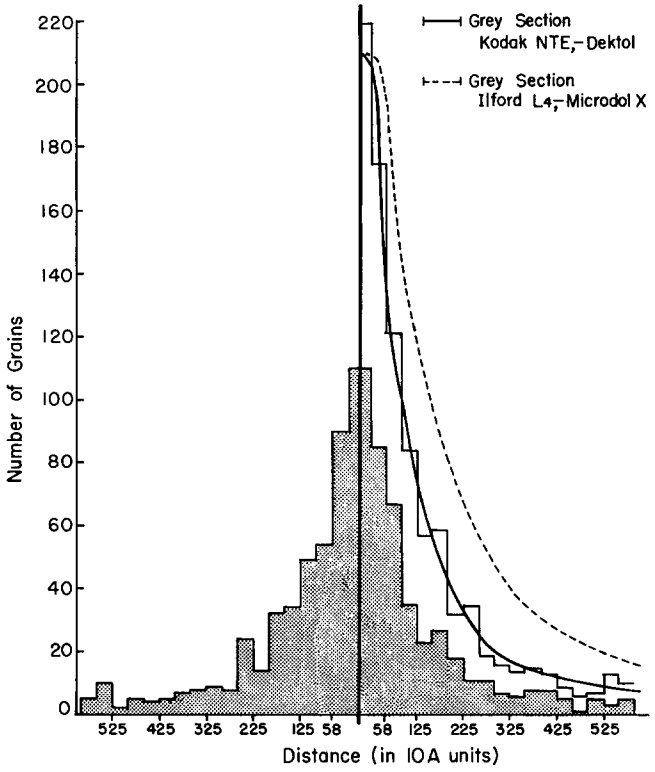

FIGURE 3 *a* Histogram of experimental density distribution around line source specimen consisting of grey section, monolayer of Kodak NTE, Dektol development. The solid line curve represents the curve of "best fit" for this histogram The dotted line represents the best fit curve for the histogram of another specimen, one consisting of grey section, monolayer of Ilford L4, Microdol X developed. Note that the shapes of the two curves are the same but that the spread is greater for the Ilford L4 specimen, and thus the resolution is poorer.

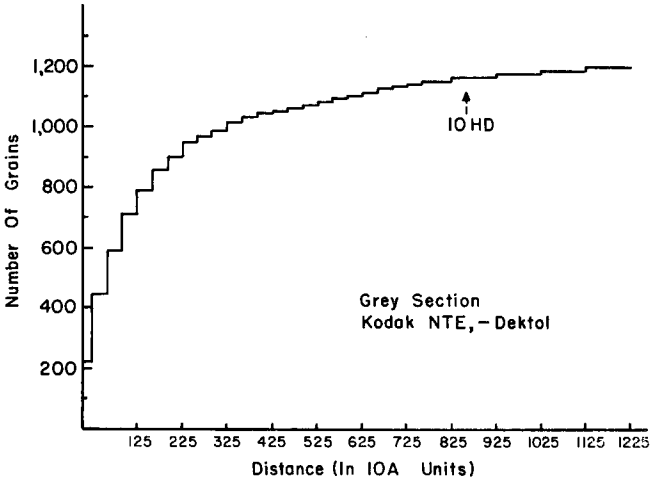

FIGURE 3 *b* Integrated grain distribution histogram for the same specimen as shown in Fig. 3 *a*, i.e. grey section, monolayer of Kodak NTE, Dektol development. The grains are added consecutively with increasing distance from the source, and thus each histogram column gives the total number of grains within this distance from the source.

over the grain, and the grain was fitted symmetrically into the smallest circle which fully circumscribed it. The center of the circle was then punched through the radioautographic print with a needle.) The measurements were done on prints at a magnification of 30,000. Grains were counted to a cut-off distance up to 2 μ on either side of the line. Background grain density far from the line was also determined.

III. RESULTS

a. Grain Distribution and Half Distance

The raw data for each specimen were treated as follows. A histogram of grain distribution from the center of the hot line was prepared in distance steps of 333 A. Since the histograms were found to be approximately symmetrical on both sides of the

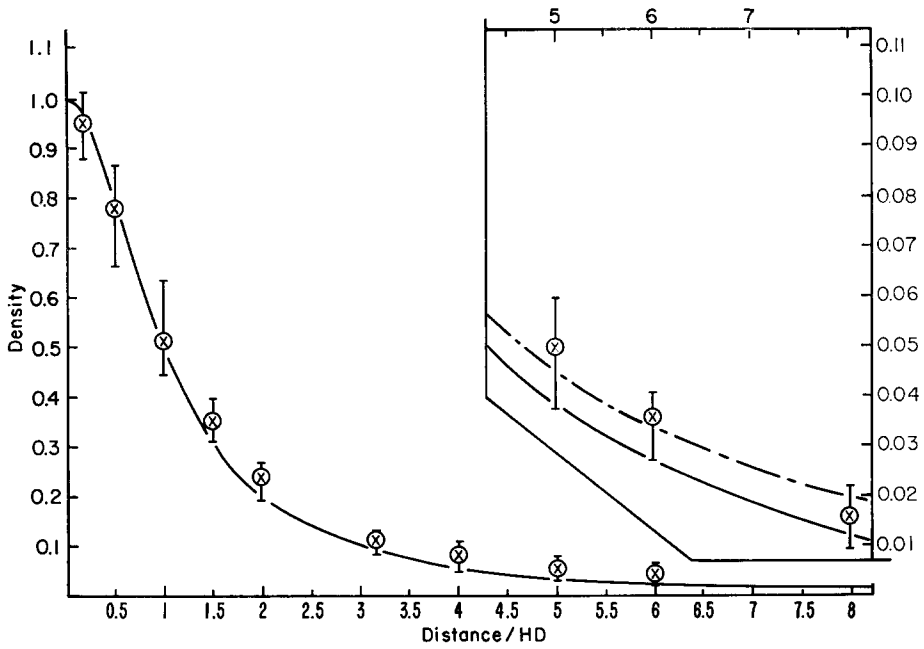

FIGURE 4 For each of a number of values for x/HD the corresponding experimental mean value of normalized density was plotted. The cross-bars represent the complete maximum range of experimental deviations from these means. Most of the experimental values fell within a considerably smaller range around the mean. The insert (in the upper right) is the tail of the same distribution with the vertical scale magnified 10 times. The experimental values are compared with a theoretical function (smooth solid curve), derived in the Appendix. The experimental and theoretical distributions fit very closely up to values of x/HD = 3. Beyond that point there is a slight discrepancy. A correction for this discrepancy is described in the Appendix and plotted in the broken curve.

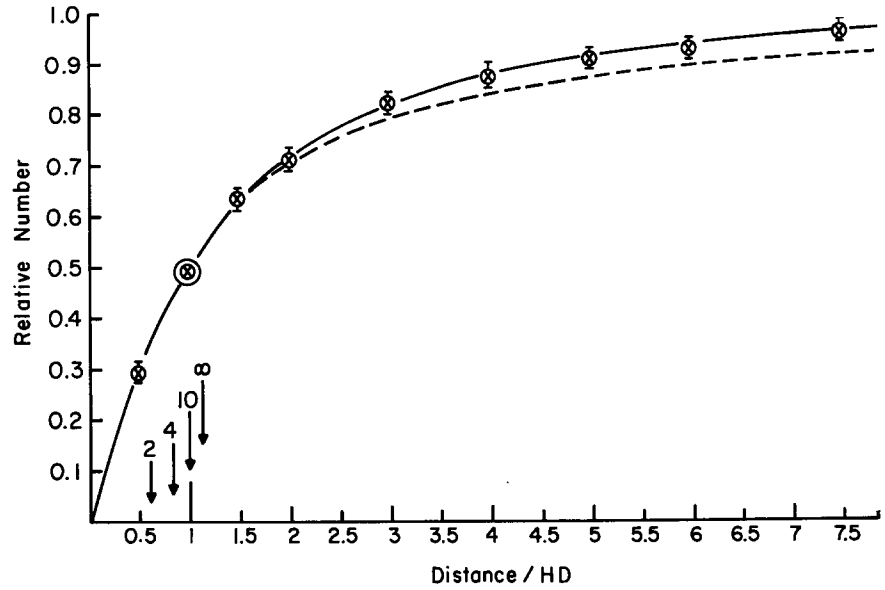

FIGURE 5 This graph plots the same data as in Fig. 4 but in integrated form. The x-axis gives distance x from the line in units of HD, the y-axis ("relative number") gives total number of grains within distance x normalized to be 1 at x = 10 HD. The mean experimental relative number with the complete range of experimental deviations (cross-bars) is shown for several values of x/HD. For (x/HD) = 1 and 10, respectively, the relative number is 0.5 and 1 by definition (the maximum experimental deviation from the mean is generally smaller than that in Fig. 4 because errors tend to be averaged out in an integrated curve). Note the excellent agreement of the experimental results with the integrated analytical function (solid curve(, also normalized to 1 at x/HD = 10. The dashed curve is the corresponding function normalized to 1 at infinity. The arrow marked 10 represents the value of HD on the basis of a cut-off distance at 10 HD, as used in the present paper. The arrows marked ∞, 4, and 2 indicate what HD would have been if the cut-off distance had been infinity, 4 HD, and 2 HD, respectively (note that HD would increase by only 12% if all grains beyond 10 HD had been included).

TABLE I

Experimental Values for Half Distance HD

Emulsion	Section	Development	HD
Ilford monolayer 1400 A	Medium gold 1200 A	Microdol X	1650
		Paraphenylenediamine	1450
	Grey 500 A	Microdol X	1450
		Paraphenylenediamine	1300
Kodak double layer 1400 A	Medium gold 1200 A	Dektol	1250
	Grey 500 A		1000
Kodak monolayer 700 A	Medium gold 1200 A		1000
	Grey 500 A		800

Values for HD were obtained experimentally and represent the distance from the radioactive line which contained 50% of the developed grains (to a cut-off distance of 10 HD). These HD values are corrected for the finite thickness of the line source (by subtracting 50 A) and are then expressed to the nearest 50 A.

Values for HD presented here are for only two section thicknesses, i.e. grey ~500 A and medium gold ~1200 A. For intermediate thicknesses HD can be extrapolated. Thus for a specimen commonly used in electron microscope radioautography (pale gold section ~1000 A, Ilford L4 and Microdol X-developed), the HD value of 1600 A is obtained by interpolation between values of 1450 for grey section and 1650 for medium gold section.

Resolution values according to the Rayleigh criterion would be 1.5 HD.

line, grains were added irrespective of sign, and one-sided histograms were plotted (e.g. Fig. 3 *a*). (For a line source, the area per histogram column remains the same with increasing distance from the source. The histograms thus represent grains per unit area, or density distributions.) A smooth curve was then fitted by eye, making sure that the differences between the curve and the histogram were as often positive as negative.

In addition to plotting a density distribution the data were tabulated in integrated form by consecutively adding the number of grains per unit distance from the line (typical example in Fig. 3 *b*). From such a tabulation, one can see what fraction of the total grains falls within a given distance from the source. The distance from the hot line within which half the developed grains fell was determined experimentally for each specimen and was called the half distance, HD. HD values for a variety of experimental conditions are tabulated in Table I.

The HD value, when properly obtained, can be a direct measure of resolution. It will be shown in subsequent sections that the HD value also provides a unit measure of distance which enables experimental radioautograms to be compared with theoretical grain distributions or "universal curves." In principle, grains could be found as far away from the line source as about 5 μ, the maximum range of tritium electrons in plastic. In practice, the bell-shaped density distribution (see Fig. 3 *a*) has fallen to very low values at distances of a few thousand Angstroms or more; the integrated distribution (see Fig. 3 *b*) rises linearly at first, then flattens and is close to its limit at a few thousand Angstroms. Thus in our specimen only a small fraction of grains is eliminated by counting grains only up to a cut-off[1] distance no larger than 2 μ.

b. Normalization and Universal Curve

The experimental curves obtained for each of the specimens listed in Table I were normalized by

[1] The numerical value that one obtains for HD decreases as one decreases the cut-off distance further. Thus, measured values of HD would have little relevance to the resolution of a specimen unless one

changing the scale on the x-axis to be 1 at a distance equal to HD (i.e. distance from the source was thus x/HD or was measured in units of HD) and by changing the scale on the y-axis to be 1 at the origin for the density distributions and to be 1 at x = 10 HD for the integrated distributions (i.e. on the integrated curve the y-axis represents the relative number of total grains within the cut-off distance of 10 HD).

When plotted on this new scale the normalized experimental curves for all the specimens tested (density or integrated) were identical within the experimental error. The averaged distributions were therefore called universal curves and are plotted in Fig. 4 and Fig. 5. These two figures, together with Table I, embody all our experimental results. In Figs. 4 and 5 the experimental distributions are compared[2] with theoretical analytical functions for a line source (converted from a previously published function for a point source, Bachmann and Salpeter, 1965; for derivation see the Appendix).

c. Sources of Error

Before exploring the applications of the universal curves, one should examine the possible sources of error and the accuracy of the experimental results. Diffusion of the dried radioactive styrene into the supporting plastic was apparently not a significant cause of error. Diffusion could be expected to proceed at different rates in Epon and methacrylate, yet the grain distribution on both sides of the line was symmetrical, the HD values being within 100 A of each other. Furthermore, no significant change in resolution was noted in preparations from the same specimen block tested a year apart. We therefore feel that a diffusion error larger than 100 A is very unlikely. The dried styrene layer was protected from organic solvents, and since it had a high molecular weight, it would not be expected to diffuse rapidly.

The finite width of the line source causes a systematic error relative to an ideal line. A correction for this effect was calculated ($\sim$50 A) and included in the data in Table I.

The error due to statistical fluctuations (because we tabulated only about 1000 grains per specimen) was theoretically estimated to be about $\pm$100 A or less. HD values from specimens with section thickness between 500 and 1200 A and from repeated tabulations on the same specimen corroborate that the statistical scatter was of the order of $\pm$100 A. Therefore, the systematic shifts in HD values with specimen thickness and photographic conditions reported in Table I, though small, are significant. A comparison with theoretical expectations will be discussed in Section V. (See also Bachmann et al., 1968.)

---

used a cut-off distance which is large compared with the true HD. In fact, if the cut-off distance is much less than the true HD, then the measured HD would be exactly one-half the cut-off distance, irrespective of the resolution or true HD of the specimen. (This appears to be the problem with the study by Miura and Mizuhira, 1965.) To obtain the values for HD presented in this study (Table I), preliminary values for HD were first obtained by tabulating grains for each specimen up to 1 μ. A final cut-off distance of 10 HD was then adopted, which was in each case less than 2 μ, and the values for HD within this new cut-off distance were obtained. These new values differ by less than 75 A from the preliminary values in each case. A cut-off distance of 1 μ would thus have been of sufficient accuracy. The cut-off distance of 10 HD was preferred merely because it facilitated subsequent mathematical manipulations of the data. It will be seen from Fig. 5 that more than 90% of all the grains are contained within the 10 HD cut-off, and that our HD values would have increased by only about 10% had all grains in the full range been counted.

[2] The agreement between the theoretical function and our experimental study strengthens our confidence in the assumptions underlying our theoretical model. One such assumption is that a developed grain *can* be formed by a single electron passing through a silver halide crystal, even though the probability of this happening is less than unity, about 20% for Kodak NTE (see Bachmann and Salpeter, 1967). We can thus rule out completely the claim advanced by Hulser and Rajewsky (1966) that a number of electrons passing through the same silver halide crystal are required to give a developed grain in fine grained emulsions such as the Kodak NTE. In our experimental study we took care that the chance of a given silver halide crystal being hit by an electron was small even immediately above the line source. If one needed "n" electrons hitting a crystal to get a developed grain, then the normalized experimental density curve would fall off with distance from the line source as the n^{th} power of our theoretical curve. If n were 5, as claimed by Hulser and Rajewsky (1966), then at 8 HD, for instance, the experimental curve would have to be lower than our theoretical one by a factor of 10^8.

IV. THEORETICAL GRAIN DISTRIBUTIONS FOR DIFFERENT GEOMETRIES

When analysing radioautograms one can plot experimental grain distributions around different cellular structures. If the expected grain distribution around such radioactive structures were known, comparison between the experimental and the theoretical distributions could reliably locate and describe the sources in the specimen. Since the grain distribution depends on both the shape and the size of the source, theoretical curves for many sources differing in geometry would be necessary to define the source accurately.

Many biological structures in thin sections can be approximated by circles or bands. We therefore restricted ourselves in the present study to considering these shapes.

a. Derivation of Curves

Since all extended sources can be considered merely as a collection of point sources, we needed first the grain distribution around a point source. We saw that a single theoretical analytic function gave a close fit to the experimental distribution around line sources, provided all distances were expressed in units of HD. This indicates that the analytic function for the distribution around a point source which corresponds uniquely to the analytic function for the line source would fit equally well (see Appendix and also Fig. 9).

The density curve around a hollow circle, Fig. 9 (a circular line source or the circumference of a circle), was obtained by numerical integration of the analytic function for a point source. (The circle was replaced by a number of points lying on the circumference. This was done separately for each of a number of radii of the circle.) Further numerical integrations gave density curves for solid circles or uniformly labeled discs, Fig. 10 (i.e. each circle was replaced by concentric hollow circles). Density curves for a hollow band (two parallel line sources), Fig. 11, were obtained by simple addition of the analytic function for line sources, and further numerical integration gave those for a solid labeled band, Fig. 12. For each density curve in Figs. 9, 10, and 12, we derived curves for relative numbers by numerical integration as described for the experimental line source. These curves are displayed in Figs. 13–15. (The integrated curves for a hollow band can easily be obtained when needed by adding the contributions from the two line sources which comprise the band.)

b. Use of the Main Curves

Figs. 9–14 are designed for the reader to use in analyzing his EM radioautograms. To do so he

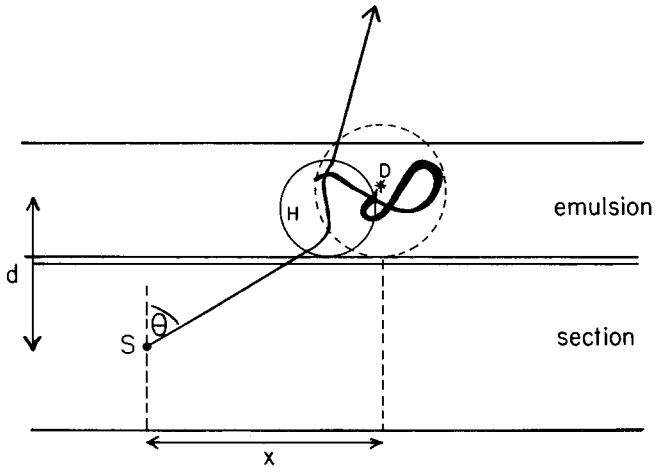

FIGURE 6 Schematic drawing of a radioautographic preparation. Radioactive sources (s) are randomly located within the biologic section; the electron (emitted at angle θ) follows an almost straight path within the section but gets scattered in the emulsion layer when it hits a silver halide crystal (H); x is the projected distance from the source (s) to a developed grain, whose position is defined as the center (D) of the smallest circumscribed circle. The resolution limiting thickness (d) of the specimen is the distance between a characteristic plane in the section and one in the emulsion.

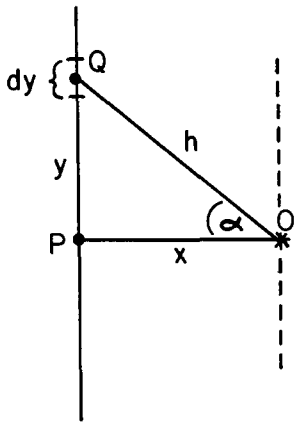

FIGURE 7 This drawing shows the relation between line and point sources. A line source can be considered as a linear collection of point sources (Q). To derive a line distribution, the line source can be subdivided into infinitely many segments of small length dy each, and each segment replaced by a point source at its midpoint. Let x be the perpendicular distance from some point of observation (O) outside the line to the line (i.e. the distance to the nearest point P on the line) and y the distance from P to one of the point sources (Q) replacing a line segment, and h the hypotenuse of the resultant triangle. The source at Q then contributes to the density at the observation point (O), an amount proportional to the point source density and to the length of line segment dy. Summing the contributions of all these segments, dy leads to an integral which gives the density function of the line source.

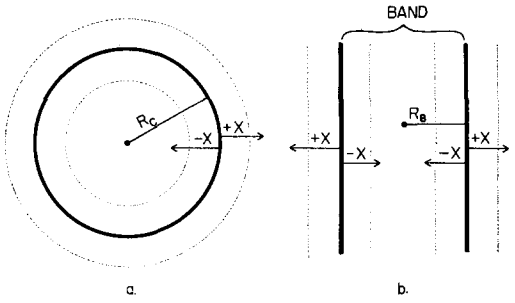

FIGURES 8 *a* and *b* Fig. 8 *a* shows the circular source of radius R_C. x defines the thickness of annuli outside (+ sign) and inside (− sign) this circle. Fig. 8 *b* shows the band source of half width R_B. Again x defines distance outside (+ sign) and inside (− sign) the source. Note that the enclosed area remains the same per unit increment in distance either inside or outside a band source, but that the enclosed area becomes progressively larger per unit increment in distance on the outside and progressively smaller inside a circular source. This must be corrected in determining density distributions, and it also explains why density distributions fall off more rapidly from circular than from band sources.

must, however, know the value for the half distance (HD) applicable to his specimen. The values for HD given in Table I were obtained experimentally for the technique introduced by Salpeter and Bachmann (1964, 1965) in which a collodion-coated glass slide provides a flat substrate for specimen mounting and emulsion coating. These HD values should, however, apply with reasonable accuracy for any technique as long as it employs tritium labeling, section thicknesses usual for electron microscopy, and closely packed, uniform emulsion layers calibrated for thickness.[3] If greater accuracy is desired, one can easily prepare a hot-line test-specimen, by following the procedures of Section II, and determine HD directly.

Once an appropriate HD value is known, even approximately, the curves can be used to test various hypotheses regarding the distribution of radioactivity in the tissue. For example, one may want to test the hypothesis that all the developed grains in a set of radioautograms come from one group of cellular structures. If in section these structures can be roughly approximated by one of four shapes, solid circle (disc), hollow circle (circumference of a circular space), solid band, or hollow band (two parallel lines), one can test this hypothesis by comparing the normalized experimental grain density distribution (tabulated in units of HD) with that predicted from the theoretical curves.

The normalized experimental grain density distribution can be obtained simply. Since one or-

[3] One physical difference between the glass-slide substrate method and others which could affect the HD value involves backscattering of electrons. We hope to report in greater detail on the effect of backscattering in a later publication. A preliminary estimate (based on experimental results by Kanter, 1957) indicates that at most 10% of the developed grains in our radioautograms are due to electrons backscattered from the glass. These backscattered electrons give a much broader distribution about the line source than do the bulk of the grains. They contribute less than 2% to the grain density at x/HD less than 1 or 2, but they increase the background slightly at large distances from the source. We have estimated mathematically that any increase in HD due to backscatter is less than 10%.

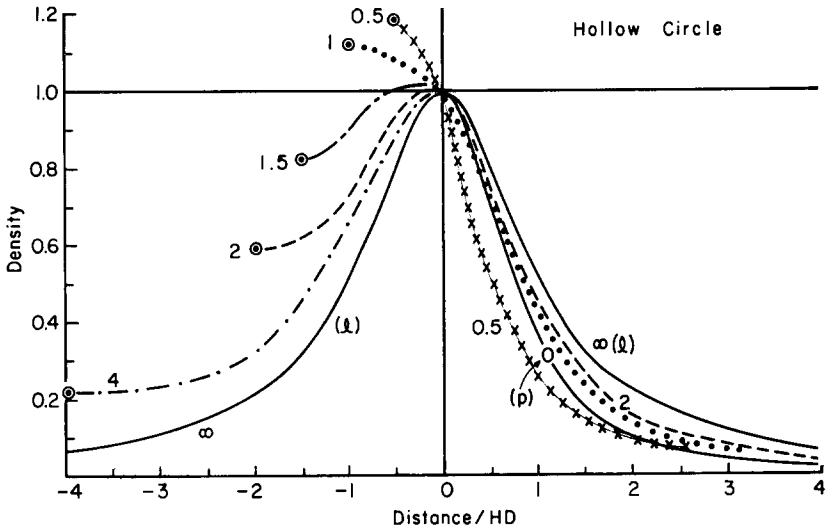

FIGURE 9 *a* Density functions for hollow circles. The x-axis represents distance in units of HD to the nearest point on the circumference of the circular source. Positive values indicate regions outside the circles; negative values indicate regions inside the circle; the zero represents points on the circumference. Each curve is labeled by the radius of the circular source (R_c) in units of HD. Density of developed grains is in each case normalized to unity on the circumference of the circular source. The limiting case of a circular source of zero radius is, of course, a point source. For finite distances from the circumference, a hollow circular source of infinite radius behaves like a line source. The density distributions for a point source and a line source are marked *p* or 0 and *l* or infinity (∞), respectively, and denote the full potential range of density distributions for hollow circular sources.

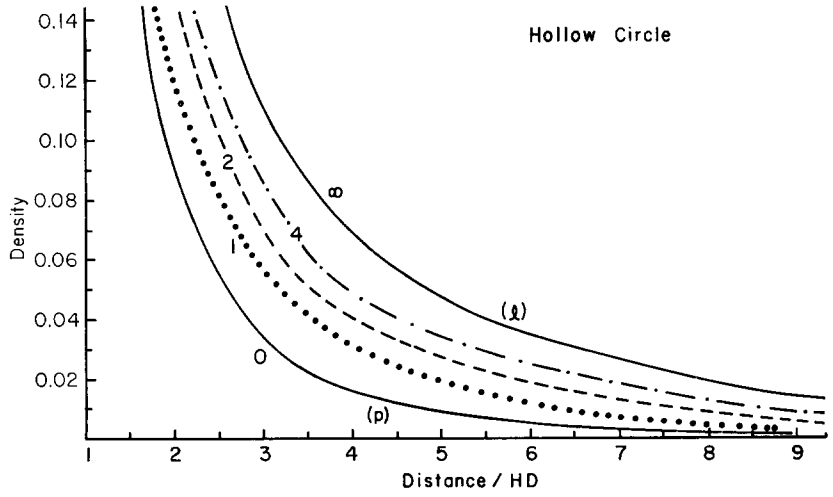

FIGURE 9 *b* Plots the tail of these curves on an expanded density scale. See Legend under Fig. 9 *a*.

ganelle or one radioautogram will not yield enough developed grains for constructing a statistically significant distribution, one has to average over a large number of randomly selected radioautograms, the assumption being that the organelles represent a homogeneous population. From this

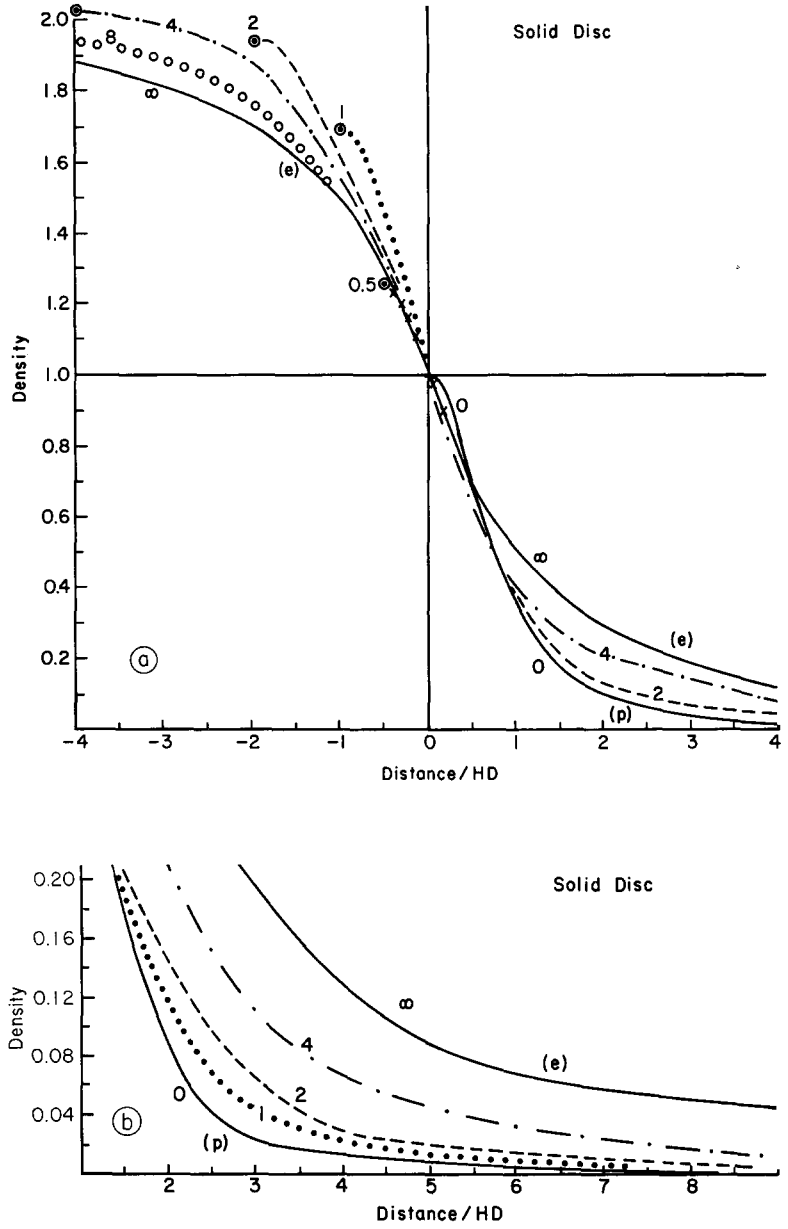

FIGURES 10 *a* and *b* Fig. 10 *a* shows density functions for sources in the form of filled circles, i.e. solid discs. In the limit of zero radius the solid disc (like the hollow circle) behaves as a point source (marked 0 or *p*). However, at finite distances from its circumference, a solid disc source of infinite radius behaves like a semiinfinite half plane with its edge at x = 0. This curve is marked ∞ or *e* (for edge). Fig. 10 *b* plots the tail of these curves on an expanded density scale. Each curve is again marked by the radius of the source in units of HD. Note by comparison with Fig. 9 that as the radius of a circle increases so does the circular difference between the shapes of the density curves on the inside of the hollow and solid circular sources. It is impossible to distinguish between hollow and solid circular sources with circles of radius 0.5 HD, but it becomes increasingly more feasible as the circle enlarges. (see Fig. 16)

sampling,[4] one first constructs a histogram of the number of grain midpoints per unit perpendicular distance from the organelle's outer edge (bounding membrane, circumference), going separately outward and inward. This histogram of grain number can be converted to a histogram of grain density simply by dividing the number of grains per "bin" of unit distance by the relative area in this bin. An easy way to obtain relative area per bin is to construct a histogram as for the developed grains but this time for a uniformly dispersed grid of points superimposed on the tabulated radioautograms. When the number of grains per histogram bin is divided by the number of points in the same bin, a density distribution is obtained no matter how irregular the shape of the object (provided enough grains and points were tabulated to give a statistically valid sample). The density histogram must next be normalized essentially by relabeling the scales on the x- and y-axis. (The x-axis becomes distance divided by estimated HD value; the y-axis becomes density divided by value in bin at the edge, i.e. density is 1 at the origin.)

The normalized density histogram is now ready for comparison with the normalized universal density curves in Figs. 9–12. The appropriate curve within each family of curves for a particular shape depends on the size of the organelle (half width, R_B, for a band and radius; R_C, for a circle) again in units of HD (averaged actual size divided by estimated HD value for the specimen) (Fig. 8). One must choose the curve closest to the experimental R_B or R_C value or interpolate between adjacent curves.

Because of the normalization, the experimental histogram and the theoretical curve will agree at the origin. The hypothesis is then tested by the goodness of the fit with distance from the origin (edge).

If one can tabulate only a small number of grains, a rough test of the hypothesis can be made by using the integrated curves (Figs. 13, 14, or 15). For each of a small number of distances x (expressed in units of HD) from the periphery, one can determine the fraction of all experimental grains (discarding any beyond 10 HD) that lie between the periphery and x. If the hypothesis is correct, this experimental fraction should be close to the value at x on the appropriate theoretical integrated curve.

From the integrated curves one can tell what percentage of total grains is expected to fall over a radioactive structure and what percentage is expected to fall outside it. This is very important for absolute quantitation (i.e. converting developed grain density to radioactive decays) or for comparing the relative radioactivity of two structures. As can be seen from Figs. 13–15, for such studies to be valid one must make a correction for scattered radiation. This is especially crucial when dealing with small structures or comparing two structures of unequal size.

From the integrated curves one can also obtain accurate probability circles (Bachmann et al., 1968). Probability circles can be used to determine simply whether a structure is significantly more radioactive than its surroundings. Such a structure would fall within a probability circle drawn around developed grains with significantly higher frequency than within the same probability circle drawn around random points.

c. Some Additional Curves

Fig. 16 plots for various sources the ratio of grain density at the center to that at the edge. This is intended to allow the reader to see more easily the minimum size of source needed before one can resolve whether the radioactivity is uniformly distributed in a structure or is restricted to the periphery. For sources with radius R_C (or of half width R_B) about 2 HD units or larger, for instance, it should be easy to distinguish a hollow from a solidly labeled source by comparing grain densities. For sources with radii (or half width) less than 0.75 HD, it is almost impossible to distinguish hollow from solid sources. For structures having radii (half width) between these two, the sources can be distinguished only if large enough samples are counted to minimize statistical fluctuations.

Various combinations of the theoretical curves can be used to generate new curves for sources not included here. For instance, for a given radius R_C of a circular source, one can generate a series of

[4] It should be emphasized that all the grain distributions assume conditions where the silver halide crystals of the emulsions are not subjected to multiple hits. Bachmann and Salpeter (1967) show that for tritium radioautography with Ilford L4 emulsion (Microdol X) a limit of four developed grains per μ^2, and with Kodak NTE emulsion (Dektol) of 20 developed grains per μ^2, is permitted to assure less than a 10% probability of multiple hits.

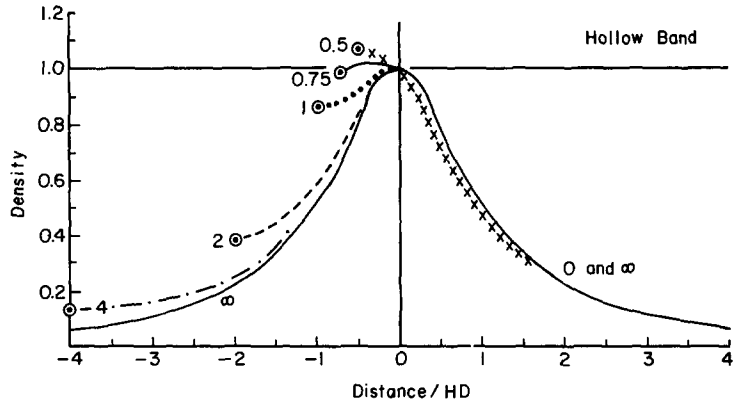

FIGURE 11 Density distributions for hollow band sources. The individual curves are labeled by half the thickness of the band (R_B) in units of HD. Positive and negative values on the x-axis indicate the outside and inside of the band, respectively, and 0 indicates the edge. The end point marked by a double ring on the left-hand side of each curve denotes the midline of the band. In the limit of zero thickness, a hollow band reduces to a line source (marked 0). For finite distances from an edge, a hollow band of infinite thickness behaves like a single line source (marked ∞). On the right-hand side the density distributions for zero and infinite thickness coincide.

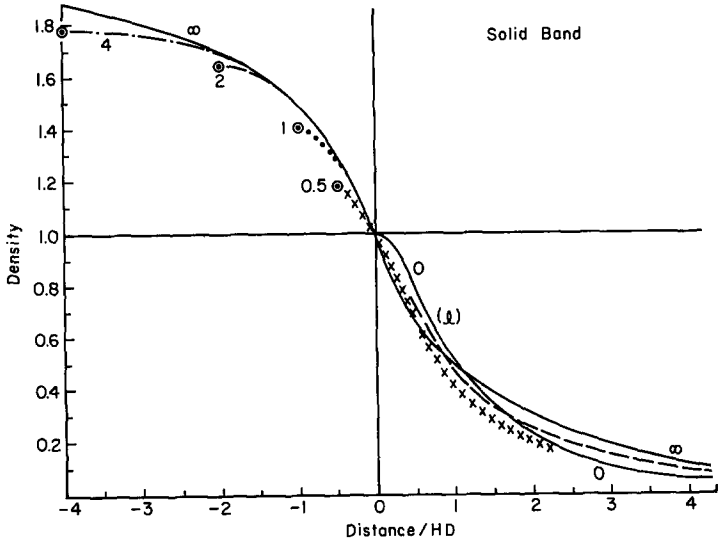

FIGURE 12 Density distributions for solid band sources. The individual curves are labeled by half the thickness of the band (R_B) in units of HD. In the limit of zero thickness, a solid like a hollow band reduces to a line source (marked 0 or l). For finite distances from an edge, a solid band of infinite thickness behaves like a semiinfinite half plane (marked ∞).

curves for conditions where there is a superimposition of label from a solid source (uniform distribution) and a hollow source (concentrated at the periphery). The density value at each of a number of points on the normalized theoretical density distribution for a solid source should be multiplied by a number q (q between 0 and 1), and the value at the same points on the distribution for a hollow source by $1 - q$. Summing these two products per point then gives a new composite curve which is also normalized to unity at the periphery. This process can be repeated for other values of q to get a composite curve that will best fit an experimental distribution which falls in shape somewhere between that for a uniformly labeled source and for a hollow source. Once the best q has been found, one can calculate the ratio (r) between the contributions from the solid and the hollow sources to

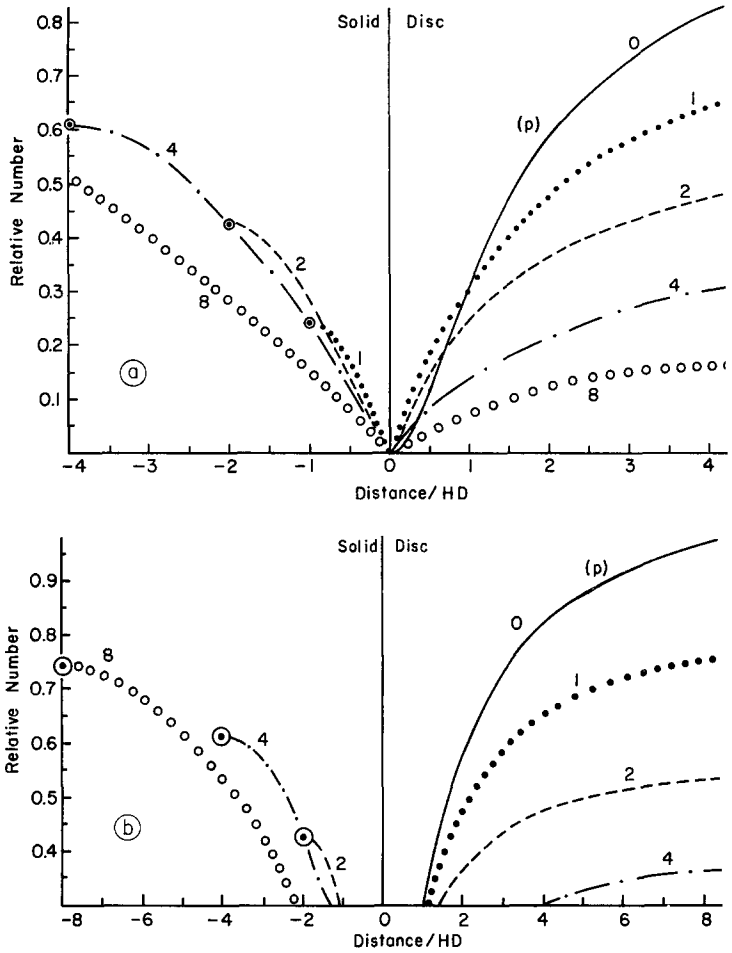

FIGURES 13 *a* and *b* Relative number (integrated) curve for uniformly labeled solid circular sources (discs). Derivation, normalization, and presentation as in Fig. 14. Fig. 13 *b* overlaps Fig. 13 *a* on a somewhat different scale.

the *total* radioactivity by substituting in the formula $r = q/(DR)(1 - q)$, where DR is an auxiliary quantity given in Fig. 17 for different radii of the source. For instance, in the companion paper (Budd and Salpeter, 1968), Fig. 1 gives an example for a circular source (sympathetic nerve ending) of radius 6 HD (0.6 μ) where a theoretical composite curve of best fit had a value of q equal to 0.70. The value of DR for this radius given in Fig. 17 is 0.4. The formula above then gives $r = 6$, i.e. the solid disc contributed about 85.7% and the hollow circle about 14.3% to the total radioactivity. (A similar rationale applies to band sources for which DR values are also given in Fig. 17.)

V. DISCUSSION

a. Definition of Resolution

There have been several discussions of resolution in EM radioautography, and there are a number of useful applicable definitions. If one has a universal curve for the density function, each definition can be expressed as a multiple of the half distance, HD.

The most common definition is the modified Rayleigh resolution distance, which was developed for light optics. It is twice the distance from a point source at which the density has fallen to half its value over the source (used by Caro, 1962). From the density curve for a point source in Fig. 9, this

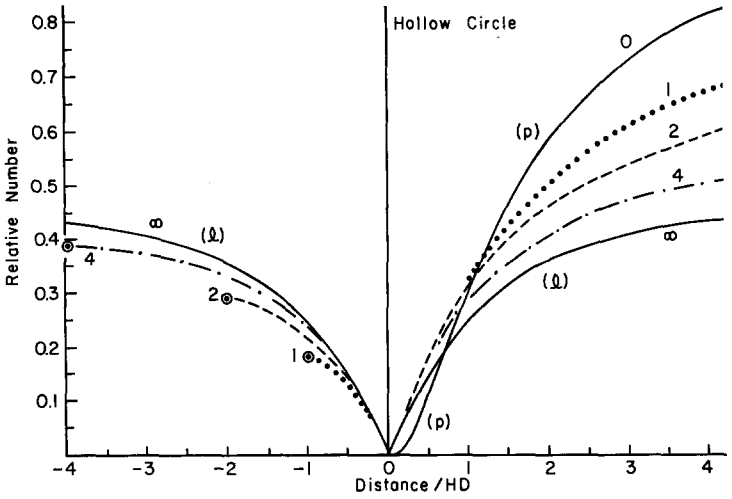

FIGURE 14 Curves for relative numbers (integrated) for hollow circular sources, derived by numerical integration of curves in Fig. 9. The value at any distance x on the positive x-axis, represents the relative number of total grains from both inside and outside the source which lie in an annulus of width around the circumference of the circular source. Values on the negative x-axis represent the relative number of total grains in an annulus of width x inside the circumference (see Fig. 8 *a*). With increasing source size, the number of grains inside the source increases relative to that on the outside. In the limiting case of infinite radius (approaching a line) the grains are equally divided between inside and outside the source (i.e. left and right of the line). The curves are all normalized to unity for the sum of grains inside plus outside the source (to 10 HD) which explains why the curves on the right side of the plot approach a different limit depending on the size of the source. The integrated distributions for a point source and a line source are marked *p* or 0, and 1 or ∞, respectively.

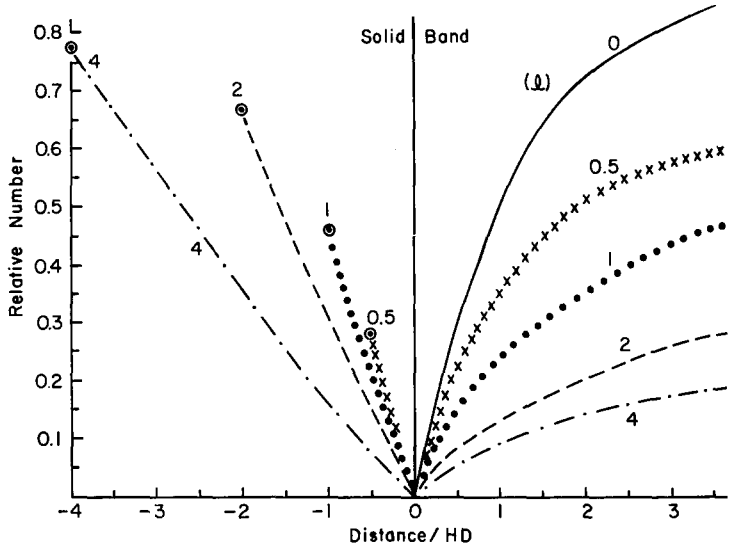

FIGURE 15 The relative numbers of total grains (integrated curve) with distance inside and outside a solidly labeled band source. The positive x-axis represents successive distances on either side outside the band, and the negative x-axis represents successive distances inside the band approaching the center line as illustrated in Fig. 8 *b*. Each curve is labeled according to the half width of the band (R_B). The limit for zero width is a single line. Since such a band of zero width has no "inside," all relative numbers are outside the source and, therefore, are plotted only on the positive x-axis, normalized to unity. Again, as the width of the source increases the relative number of grains outside it decreases.

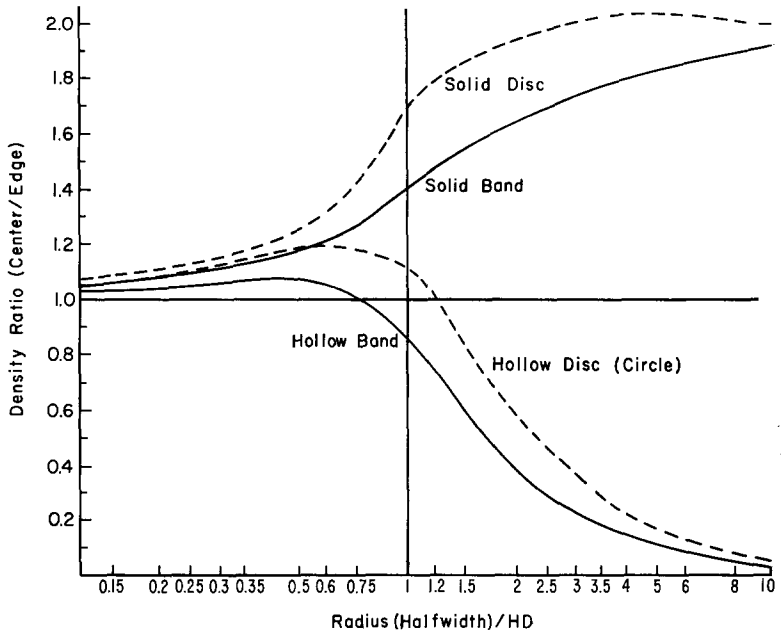

FIGURE 16 Ratio of density in the center of solid or hollow circular (or band) sources over that at the edge of the same source as a function of increasing radius (half width) in units of HD. It is clear that one cannot distinguish between hollow or solid sources for structures of radius (half width) less than 0.75 HD.

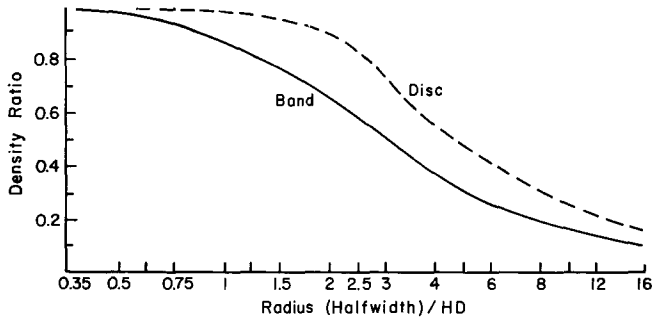

FIGURE 17 Assuming that half the total radioactivity of a source is uniformly distributed throughout the source and that the other half is all concentrated at the periphery, then the over-all grain density will be a composite of the contributions from these two components. The ratio of density due to the uniformly distributed "solid" source over that due to the hollow source at the periphery is called DR and is plotted in this figure for both a circular (disc) and a band source as a function of source radius (half width).

resolution distance is 1.5 HD. Resolution distances by this 50% density criterion differ for sources differing in geometry, e.g. it is just over 2 HD for a line source (see Fig. 9).

Bachmann and Salpeter (1965) introduced another useful resolution criterion in terms of the distances from individual developed grains with given probability of containing a point source. It should be remembered that the distance from a developed grain with, for instance, a 50% probability that it contains a point source is also the distance from (i.e. radius of circle around) a point source within which 50% of the total grains fall. These probability distances can be obtained from the integrated curves (relative number) for point sources in Fig. 13.

Circles of radii 0.85 HD, 1.7 HD, and 3.2 HD have a probability of 25%, 50%, and 75% of

containing a point source (see also Bachmann et al., 1968). The circle of probability 50% is for a point source what HD is for a line source and will be called "HR", corresponding roughly to E_t obtained theoretically by Bachmann and Salpeter (1965) in different units.

While the distance from the source within which half the grains fall is considerably *larger* for a point source (HR), Fig. 14, than for a line source (HD), Fig. 15, the density distribution falls off *more rapidly* for the point than for the line source (see Fig. 9 *a*). This contrast illustrates the difference in shapes of the grain distributions around a point source and a line source.[5] Thus, if one used density as a measure of resolution, a point source would give a more favorable value than a line source; but the inverse holds if the relative number of grains within a given distance from the source is the criterion for resolution. This emphasizes the inadequacy of judging resolution by a single value assigned to a specimen or technique without a clear understanding of how this is related to the full grain distribution.

b. Comparison with Previous Results

The first critical study on resolution in EM radioautography is that of Caro (1962). He carried out a numerical calculation for a simple theoretical model based on assumptions somewhat similar to ours. There is, however, a discrepancy between us in the theoretical density distribution for a point source (compare Caro, 1962, Fig. 4, with this study, Fig. 6, curve marked *p*). Caro's curve falls off more rapidly than does ours, especially at the beginning of the curve. The value for resolution according to the modified Rayleigh (50% density) criterion is about a factor of two smaller on Caro's curve than on ours. One cause for the discrepancy in the theoretical distributions comes from the fact that Caro's density curve starts decreasing at the origin with a large finite slope, whereas ours is horizontal at the origin (i.e. zero slope, bell-shaped curve). A general symmetry argument shows that the slope must be zero at the origin. The density distribution is symmetrical around the origin, i.e. it falls off with a negative slope on one side and a positive slope on the other. Therefore, the slope must change sign at the origin, i.e. it must have a zero value or a horizontal slope there. If one arbitrarily rounds off the curve presented by Caro (1962, Fig. 4) at small values of x, then his and our curves agree better (the value for resolution according to the Rayleigh criterion depends directly on the density value at the origin).

Caro also presents an experimental histogram of grain distribution around virus particles and bacteria (Caro, 1962; Caro and Schnos, 1965) which fits his theoretical curves. Since these studies are of obvious high quality, we are at a loss to explain the discrepancy between these experimental distributions and ours.

Miura and Mizuhira (1965) obtained a value of 575 A for some measure of resolution from an integrated function of grain distribution around a tritium-labeled virus particle. They, however, counted grains only up to 1200 A. As was discussed in Section III and footnote 1, this cut-off distance is much too short to give a meaningful value for resolution. Lettre and Paweletz (1966) give some theoretical discussion of resolution and experimental illustrations for improved resolution with decreasing developed grain size. Their theoretical discussion shows no consideration for the geometry of the specimen, and the experimental illustrations lack statistical verification or any convincing argument. A brief theoretical discussion with a predicted value for resolution was given by Coimbra and Leblond (1966). However, this value did not take into consideration specimen thickness, and an incorrect value for range was used. The correct range in plastic in which the electron originates is 0.8 μ mean and 5 μ maximum (Bethe and Ashkin, 1953).

Bachmann and Salpeter (1965) derived a formula, based on a simplified theory for geometric and photographic error, for a quantity E_t

[5] The difference in the distribution for relative numbers stems mainly from the fact that the measured "distance" is the actual distance to a point source, whereas for a line source it is always the shortest perpendicular distance (x) to the line. Yet the real source may be anywhere along the radioactive line, and the actual distance (h) is accordingly longer (see Fig. 7). The difference in the density distributions, on the other hand, is related to the fact that distance from a point source gives circles whose area is proportional to the square of the distance (radius); whereas from a line source, it gives bands whose area is linear with the distance (width). Since density expresses grains per unit area, it falls off more rapidly for the point source (see also Fig. 8 and Appendix).

such that $E_t/1.7$ should equal the half distance HD for a line source. These theoretical estimates for HD are smaller than our experimental values by 5–30%, the discrepancy being smallest for Kodak NTE developed with Dektol, and largest for Ilford L4. This suggests that the theoretical formula underestimates some photographic factor which might be "grain movement" during development. Bachmann and Salpeter (1965) showed that grain movement is potentially greater with Ilford L4. When Kodak NTE was developed with Elon ascorbic acid after gold latensification (Salpeter and Bachmann, 1964) the resultant HD values were larger than those when Dektol is the developer (1000 A and 1400 A for grey sections and medium gold sections, respectively). The long developing time and the absence of hardening salts in the Elon-ascorbic acid development used by us may have led to appreciable grain movement. We therefore do not recommend this developing procedure until possible improvements have been investigated.

Although there still are obvious puzzles regarding the exact values of HD, it should now be possible to estimate HD to well within a factor of two for a wide variety of controlled experimental conditions. The introduction of HD as a unit of normalization in conjunction with the universal curves should provide greater flexibility in the analysis of EM radioautograms.

Mathematical Appendix

This appendix gives the mathematical derivations of the theoretical functions. It is not necessary either for the understanding of the main text or for the use of the theoretical curves.

Consider first a point source embedded in a methacrylate section with a horizontal emulsion layer lying on top of the section. Let d be the distance along the vertical line from the source to the horizontal midplane of the emulsion (the shortest distance from the point to the plane), and let θ be the angle between this vertical d line and the direction of emission of an electron (Fig. 6). Electrons are emitted in random directions. Of all the electrons which are emitted upwards, that fraction (called relative number) which travel within a cone of half angle θ about the vertical is equal to $1 - \cos\theta$. If the emitted electrons travelled in a straight line this relative number of electrons ($1 - \cos\theta$) would hit the midplane of the emulsion within a circle (centered about a point vertically above the source) of radius $x = d \tan\theta$. Let us also define the relative number of developed grains within this circle of radius x as $F_p(x)$. If one could neglect all photographic errors, i.e. if the center of a developed grain appeared exactly where the electron hits this plane, then $F_p(x)$ would be equal to $1 - \cos\theta$. Using the trigonometrical identity,

$$\cos\theta = \frac{1}{(1 + \tan^2\theta)^{1/2}} \tag{1}$$

one can reexpress the relation

$$F_p = 1 - \cos\theta \tag{2 a}$$

as

$$F_p(x) = 1 - \frac{1}{[1 + (x/d)^2]^{1/2}}. \tag{2}$$

Essentially this formula for the relative number F_p of grains within distance x from a point source (the "integrated curve") is plotted in Fig. 13 in the curve labeled p, except that, as in all curves of the present paper, distance along the x-axis is measured in units of an empirical length HD rather than in units of d. This formula for F_p, as well as for the density distribution function f_p, was derived in Bachmann and Salpeter (1965) in terms of the angle θ. Using the identity

$$x = d \tan\theta, \qquad \theta = \arctan(x/d) \tag{3}$$

one can, of course, reexpress their formula for f_p in terms of x. For the sake of completeness, we rederive this formula directly in terms of x. In our present notation we consider a thin annulus (width dx) surrounding a circle of radius x. The area of such an annulus is $2\pi x\,dx$. The relative number of developed grains within this annulus is

$$\frac{dF_p}{dx}\,dx = \frac{1}{[1 + (x/d)^2]^{3/2}} \times \frac{x}{d^2} \times dx. \tag{4}$$

The grain density f_p is simply this small relative number of grains divided by the small area ($2\pi x\,dx$) of the annulus, except for a multiplicative "normalization factor." We chose this factor so to make f_p unity at $x = 0$, which gives

$$f_p = \frac{1}{[1 + (x/d)^2]^{3/2}}. \tag{5}$$

Using equations 1 and 3 this can be reexpressed as

$$f_p = \cos^3\theta \tag{5 a}$$

which is the expression in Bachmann and Salpeter (1965).

Once one has a known analytic function f_p for the grain density distribution around a point source, one can derive the equivalent density distribution f_l around a line source, as follows. Subdivide the line source into infinitely many segments of small length dy each, and replace each segment by a point source at its midpoint as shown in Fig. 7. Let x be the perpendicular distance from some point of observation outside the line to the line (i.e. the distance to the nearest point (P) on the line) and y the distance from P to one of the point sources (Q) replacing a line-segment and h the hypotenuse of the resultant triangle $= (x^2 + y^2)$. The source at Q then contributes to the density at the observation point an amount proportional to the point source density evaluated for $h[f_p(h)]$. Summing the contributions of all these segments, dy, leads to an integral,

$$f_l \propto \int_{-\infty}^{+\infty} f_p(\sqrt{x^2 + y^2})\, dy. \tag{6}$$

To normalize this density distribution f_l around a line source to unity at the origin, one divides the value of this integral at each x by its value at $x = 0$. For the particular form of f_p given in equation 5, these integrals can be evaluated analytically and lead to

$$f_l = \frac{1}{[1 + (x/d)^2]}. \tag{7}$$

This is the density function for a line source discussed in Section III (Fig. 4). Using equations 1 and 3 this can be rewritten as

$$f_l = \cos^2 \theta. \tag{7 a}$$

The relative number F_l of grains within perpendicular distance x from a line source can be obtained from the density function f simply by integration,

$$F_l(x) \propto \int_0^x f_l(x')\, dx', \tag{8}$$

where x' is the running variable between zero and x. If one divides this integral for every value of x by the value of this integral at $x = \infty$, one obtains the relative number F_l normalized to unity at infinity (if only grains up to some finite cut-off distance X were to be considered, one would instead divide by the value of the integral at x equal to X). For the special form in equation 6 for f_l, the integrals can again be evaluated analytically and lead to

$$F_l = \frac{2}{\pi} \arctan \frac{x}{d}. \tag{9}$$

Essentially this expression for the relative number F_l for a line source is plotted in the dashed curve in Fig. 5. Using equations 1 and 3 this can be rewritten as

$$F_l = \frac{2}{\pi}\theta. \tag{9 a}$$

The model we have outlined gives a qualitative picture of the geometric factors for point sources and for line sources. The line source density function f_l in equation 7 is simply $1/[1 + Z^2]$ where $Z = x/d$. The solid curve in Fig. 4 compares this function with the experimental points, (in this curve Z equals distance divided by the empirically determined HD). The agreement is excellent for Z appreciably less than about 4 or 5, but the function is systematically slightly too low for Z above about 4 or 5. By trial and error we found an empirical correction to our theoretical functions. Instead of equation 5 we use

$$f_p = \frac{0.9964}{[1 + Z^2]^{3/2}} + \frac{0.45}{[25 + Z^2]^{3/2}}, \tag{5 b}$$

and further integration and normalization gives instead of equation 7

$$f_l = \frac{0.982}{1 + Z^2} + \frac{0.45}{25 + Z^2}. \tag{7 b}$$

This last expression (7 b), shown as the broken curve in the enlarged insert of Fig. 4, agrees better with the experimental points. (In the main curve of Fig. 4 the difference would hardly be noticeable.) In constructing the curves for other kinds of sources in the later figures in this paper, we used equation 5 b instead of 5, thus providing the slight correction at the tail of the distributions.

We wish to thank Mrs. Frances McHenry and Mrs. Maria Szabo for technical assistance.

This work was supported in part by United States Public Health Service Research grant No. GM 10422-06 from the Division of General Medical Sciences and by Career Development Award No. NB-K3-3738 from the Division of Neurological Diseases and Blindness (awarded to Dr. M. M. Salpeter) and by a contract with the Office of Naval Research (awarded to Dr. E. E. Salpeter).

Received for publication 14 June 1968, and in revised form 28 October 1968.

Note Added in Proof: With tritium-labeled specimens as used in E. M. radioautography, absorption and scattering act to improve resolution. In such thin specimens electrons from ^{14}C already have enough

energy to effectively travel in straight lines with little absorption and scattering. Thus, unlike the situation in light microscope radioautography where relatively thick specimens are used, the resolution for E. M. radioautographs should get slightly worse when going from tritium labeling to ^{14}C and then remain almost unchanged when going to isotopes of even higher energy.

Since the submission of this manuscript we have obtained preliminary experimental results for a line source of polystyrene-^{14}C. The HD values are slightly larger than with tritium (by factors of less than 2).

REFERENCES

BACHMANN, L., and M. M. SALPETER. 1965. Autoradiography with the electron microscope: a quantitative evaluation. *Lab. Invest.* **14**:1041.

BACHMANN, L., and M. M. SALPETER. 1967. Absolute sensitivity of electron microscope radioautography. *J. Cell Biol.* **33**:299.

BACHMANN, L., M. M. SALPETER, and E. E. SALPETER. 1968. Das Auflösungsvermögen elektronen-mikroskopischer Autoradiographien. *Histochemie.* **15**:234.

BACHMANN, L., and P. SITTE. 1958. Dickenbestimmung nach. Tolansky an ultradunnschnitten. *Mikroskopie.* **13**:289.

BETHE, H. A., and J. ASHKIN. 1953. Passage of radiation through matter. *In* Experimental Nuclear Physics. E. Segre, editor. John Wiley & Sons, Inc., New York. **1**:166–357.

BUDD, G. C., and M. M. SALPETER. 1968. The distribution of labeled norepinephrine within sympathetic nerve terminals studied with electron microscope radioautography. *J. Cell Biol.* **41**:21.

CARO, L. G. 1962. High resolution autoradiography. II. The problem of resolution. *J. Cell Biol.* **15**:189.

CARO, L. G., and M. SCHNOS. 1965. Tritium and phosphorus-32 in high resolution autoradiography. *Science.* **149**:60.

CARO, L. G., and R. P. VAN TUBERGEN. 1962. High resolution autoradiography. I. Methods. *J Cell Biol.* **15**:173.

COIMBRA, A., and C. P. LEBLOND. 1966. Sites of glycogen synthesis in rat liver cells as shown by electron microscope radioautography after administration of glucose-H^3. *J. Cell Biol.* **30**:151.

DONIACH, I., and S. R. PELC. 1950. Autoradiograph technique. *Brit. J. Radiol.* **23**:184.

GRANBOULAN, P. 1963. Resolving power and sensitivity of a new emulsion in electron microscope autoradiography. *J. Roy. Microsc. Soc.* **81**:165.

HULSER, D. F., and M. F. RAJEWSKY. 1966. Characteristics of three nuclear emulsions for autoradiography at the electron microscope. *Biophysik.* **3**:123.

KANTER, W. 1957. Zur Ruckstreuung von Elektronen im Energiebereich von 10 bis 100 KeV. *Ann. Physik.* **20**:144.

LAMERTON, L. F., and E. B. HARRIS. 1954. Resolution and sensitivity in autoradiography. *J. Photographic Sci.* **2**:135.

LETTRE, H., and N. PAWELETZ. 1966. Probleme der elektronenmikroskopischen autoradiographie. *Naturwissenschaften.* **53**:269.

LIQUIER-MILWARD, J. 1956. Electron microscopy and radioautography as coupled techniques in tracer experiments. *Nature.* **177**:619.

MIURA, T., and V. MIZUHIRA. 1965. Determination of autoradiographic resolution by ^3H- or ^{32}P labelled RNA phages in electron microscopy. *J. Electron Microscopy (Japan).* **14**:327.

PEACHEY, L. D. 1958. Thin sections. I. A study of section thickness and physical distortion produced during microtomy. *J. Biophys. Biochem. Cytol.* **4**:233.

PELC, S. R. 1963. Theory of electron autoradiography. *J. Roy. Microsc. Soc.* **81**:131.

SALPETER, M. M. 1966. General area of autoradiography at the electron microscope level. *In* Methods in Cell Physiology. D. Prescott, editor. Academic Press Inc., New York. **2**.

SALPETER, M. M., and L. BACHMANN. 1964. Autoradiography with the electron microscope. A procedure for improving resolution, sensitivity and contrast. *J. Cell Biol.* **22**:469.

SALPETER, M. M., and L. BACHMANN. 1965. Assessment of technical steps in electron microscope autoradiography. *In* Use of Radioautography in Investigation of Protein Synthesis. C. P. Leblond and E. Warren, editors. Academic Press Inc., New York. 23.

STEVENS, A. R. 1966. High resolution autoradiography. *In* Methods in Cell Physiology. David M. Prescott, editor. Academic Press Inc., New York. **2**.

STEVENS, G. W. W. 1950. The radioactive micrographs for resolution testing in autoradiography. *Brit. J. Radiol.* **23**:723.